

AD-A257 275



WHOI-92-26

2

**Woods Hole  
Oceanographic  
Institution**



---

**Particle Contact on Flat Plates in Flow:  
A Model for Initial Larval Contact**

by

Elizabeth D. Garland and Lauren S. Mullineaux

June 1992

**Technical Report**

Funding was provided by the Office of Naval Research  
under Contract Nos. N00014-89-J-1431 and N00014-89-J-1112.

Approved for public release; distribution unlimited.

---

**DTIC**  
**ELECTE**  
**NOV 17 1992**  
**S E D**

82 11 16 045

92-29602



**WHOI-92-26**

**Particle Contact on Flat Plates in Flow:  
A Model for Initial Larval Contact**

by

**Elizabeth D. Garland and Lauren S. Mullineaux**

**Woods Hole Oceanographic Institution  
Woods Hole, Massachusetts 02543**

**June 1992**


**Technical Report**

**Funding was provided by the Office of Naval Research  
under Contract Nos. N00014-89-J-1431 and N00014-89-J-1112.**

**Reproduction in whole or in part is permitted for any purpose of the United States  
Government. This report should be cited as Woods Hole Oceanog. Inst. Tech. Rept.,  
WHOI-92-26.**

**Approved for public release; distribution unlimited.**

**Approved for Distribution:**



---

**Joel C. Goldman, Chairman  
Department of Biology**

# Contents

List of Figures .....	2
List of Tables .....	2
1 Introduction .....	3
2 Methods .....	4
2.1 Plate Design and Flow Measurements .....	4
2.2 Particle Contact Experiments .....	5
2.3 Statistical Analyses .....	9
3 Results .....	10
3.1 Flow Over Plates .....	10
3.2 Particle Concentrations in the Flume .....	13
3.3 Particle Contact Patterns .....	13
3.4 Particle Contact Rates .....	20
4 Discussion .....	21
4.1 Particle Contact Patterns in a Developing Boundary Layer .....	21
4.2 Implications for Larval Settlement .....	22
4.3 Particle Contact Rates in Non-Varying Flow .....	23
4.4 Interpretation of Larval Settlement Plates .....	24
5 Acknowledgements .....	25
6 Literature Cited .....	25

DTIC QUALITY INSPECTED 4

Accession For	
NTIS	CRA&I <input checked="" type="checkbox"/>
DTIC	TAB <input type="checkbox"/>
Unannounced <input type="checkbox"/>	
Justification .....	
By .....	
Distribution / .....	
Availability Codes	
Dist	Avail and/or Special
A-1	

## List of Figures

Figure 1. Plate design and qualitative boundary layer flow patterns .....	4
Figure 2. Design of the paddle wheel flume .....	6
Figure 3. Quantitative flow measurements over experimental plates .....	11
Figure 4. Particle concentrations in the flume during replicate runs .....	13
Figure 5a. Particle contact patterns on faired plates .....	14
Figure 5b. Particle contact patterns on bluff plates .....	15
Figure 5c. Particle contact patterns on split plates .....	16
Figure 6. Particle contact rates on faired, bluff and split plates .....	21
Figure 7. Particle contact rate as a function of along-stream flux .....	21

## List of Tables

Table 1. Particle concentration in replicate flume runs .....	17
Table 2. Kendall's $\tau$ correlation between particle contact and flow .....	17
Table 3. F ratios from ANOVA of cross-stream particle abundances .....	19
Table 4. F ratios from ANOVA of downstream particle abundances .....	20

# 1 Introduction

Predicting locations where particles will first contact a flat surface is possible in steady, unidirectional, boundary-layer flows by using momentum flux as an analog to particle flux (e.g., Schlichting, 1979). Predicting particle behavior in flows over complex surfaces is more difficult (Paola, 1983; Middleton and Southard, 1984). Particle contact with a surface in flow is determined by particle characteristics, such as size, density and sinking velocity, and flow characteristics such as free-stream flow velocity, turbulence, shear stress and flow separations in the boundary layer. Hydrodynamic processes that determine particle contact with a surface also may influence initial settlement of benthic invertebrate larvae in controlled laboratory flows (Hannan, 1984; Butman, 1986, 1987; Mullineaux and Butman, 1991) and in the field (Duggins et al., 1990; Keen, 1987; Mullineaux and Butman, 1990; Mullineaux and Garland, in prep). It is often difficult, however, to determine which flow characteristic is responsible for the resulting settlement pattern. Furthermore, the post-contact exploratory behavior of larvae can also cause deviations from settlement patterns expected from hydrodynamic considerations alone.

The utility of using the flat plate approach in controlled laboratory flows is that different configurations of the leading edge of flat settlement plates allow alteration of boundary-layer flows without changing the character of the surface. Leading edges can be constructed to generate a variety of boundary-layer flows differing in boundary-layer thickness, turbulence, plate-ward advection, and shear stress. Although these characteristics co-vary downstream from the leading edge in a classical boundary layer over a thin flat plate, they do not always co-vary in flows over more complex surface geometries. In some of these cases, each flow characteristic can be isolated, and its effects studied independently. Because movements of relatively small particles are strongly influenced by flow (e.g., Nowell, 1983), sites and rates of initial contact onto plates should be predictable from boundary-layer flow characteristics. Contact of particles with plates in these flows is, in turn, a useful analog for initial contact of passive larvae onto similar surfaces.

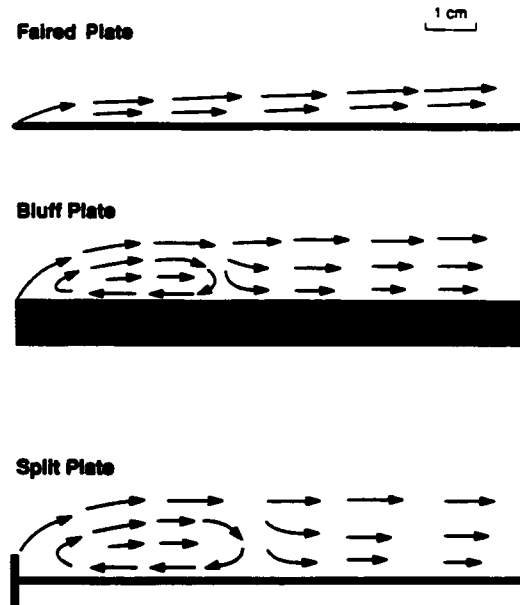
The objective of the present study was to quantify: (1) the location, relative to the leading edge, where small, low-density particles first contact a flat surface in a developing boundary layer (based on varying downstream turbulence, shear stress and vertical advection); and (2) the relationship between contact rate of particles on flat surfaces and particle flux parallel to the surface in a uniform, fully-developed, boundary layer. These contact rates and patterns were then used to model initial contact of passive larvae and propagules onto flat plates. Relatively small ( $< 100 \mu\text{m}$ ), low-density larvae are the focus of this study for two reasons: (1) they are more likely to be passive in boundary-layer flows than large larvae because their swimming speeds tend to scale with their size; and (2) small larvae, hydrodynamically similar to the particles used in this study, are prominent in the deep sea (Mullineaux, 1992) where these models will be tested. This study was designed to help define the role of flow in larval contact and settlement onto natural surfaces in deep-sea habitats and for evaluating collection characteristics of larval settlement plates. If, for example, larval contact rates can be predicted from larval concentration in controlled laboratory flume flows, then settlement rates onto plates can be used to estimate quantitative larval abundances in the field, assuming that larvae initially contact plates like passive particles (Mullineaux and Butman, 1991).

## 2 Methods

### 2.1 Plate Design and Flow Measurements

In order to correlate particle contact onto surfaces with specific flow characteristics, flat plates were constructed with three types of leading edge configurations: "faired", "bluff", and "split" (Fig. 1). Each leading edge configuration generated unique boundary-layer flows that could be used to determine flow characteristics that may be responsible for influencing particle contact with plates. All three plates were 10 cm wide by 26 cm long and were constructed from polycarbonate plastic sheets.

**Figure 1.** Plate design and qualitative velocity vectors drawn from LDV measurements of vertical and horizontal velocities at a along-stream flow speed of  $10 \text{ cm s}^{-1}$  (measured at 10 cm above flume bottom). Flume flow is from left to right in diagram.



The three plate types were configured to develop the boundary layer flows described in Mullineaux and Butman (1991). The "faired" plate was 0.15 cm thick along its entire length, with the leading edge tapered to create a fairing for the oncoming flow. A classical boundary layer, described by "flat plate" theory (e.g., Schlichting, 1979) was expected to develop along this plate. The "bluff" plate was 1.0 cm thick along its length. Over this plate, the flow was expected to separate at the bluff surface of the leading edge and reattach downstream at a location determined by the along-stream velocity and leading edge thickness (Ruderich and Fernholz, 1986). The "split" plate was 0.15 cm thick along its length but had a "splitter bar", consisting of a 1.0 cm high polycarbonate strip attached normal to the flow, at the leading edge. Flume studies (Mullineaux and Butman, 1991) showed that the flow separation created by this configuration was qualitatively similar to that of the bluff plate, but differed in size and turbulent intensity. In addition, the splitter bar caused the mean horizontal velocity and shear stress immediately downstream of the leading edge to be substantially reduced relative to similar locations on the bluff and faired plates.

Flow over the three plate types was measured using a two-axis, forward-scatter laser Doppler velocimeter (Agrawal and Belting, 1988). The plates were set up individually for LDV measurements in an open-channel flow (see Butman and Chapman [1989] for a description of the flume and Mullineaux and Butman [1991] for a detailed description of profiling above a flat plate using the LDV). The flume was 17 m long and 60 cm wide, with an experimental "test section" located 12 m downstream from the flow straighteners. The flume was filled with freshwater to a height of 12 cm and the flow was adjusted to one of the two flow speeds ( $5$  or  $10 \text{ cm s}^{-1}$  at 10 cm above the flume bottom).

Single plates were placed in the flume at the center of the test section, with the plate edges 25 cm from the flume side-walls. The plates were elevated 5 cm above the flume bottom on thin plastic legs in order to raise them above the region of highest shear within 2-3 cm of the bottom. Plates were oriented horizontally with their long dimension parallel to the flow. Vertical velocity profiles were measured with the LDV at successive locations downstream from the leading edge. The two axes allowed for simultaneous measurements of instantaneous along-stream ( $u$ ) and vertical, or plate-ward ( $w$ ) velocities. Velocity means ( $\bar{u}$ ,  $\bar{w}$ ), standard deviations [ $\text{rms}(u')$ ,  $\text{rms}(w')$ ], and variances ( $u'^2$ ,  $w'^2$ ) were calculated from measurements taken for 4 minutes at each position. Turbulence [ $\text{rms}(w')$ ] and mean vertical advection ( $w$ ) were calculated by integrating over the boundary layer from measurements taken at eight heights between 0.1 and 2.0 cm above the plate, as in Mullineaux and Butman (1991). Shear stress was calculated from the turbulent kinetic energy ( $u'^2$ ) at a height of 0.1 cm above the plate. The downstream locations and spacing of profiles varied slightly among plate types and flow speeds, and depended on the presence and location of flow separation and reattachment points. No velocity profiles were measured over plates at  $2 \text{ cm s}^{-1}$  flows because of limitations of the flume pump at slow speeds. Instead, dye was released at the leading edges of the plates at an along-stream flow speed ranging from 2 to  $13 \text{ cm s}^{-1}$ , in order to visualize flow separations and the boundary-layer thickness. These studies were useful for determining critical flow speeds for development and destabilization of flow separations over each plate.

## 2.2 Particle Contact Experiments

Particle contact experiments were performed using the same experimental plates but in a different flume (Fig. 2). A racetrack-style flume (the Paddle-Wheel Flume described in detail in Butman and Grassle, submitted) was chosen for the particle contact studies because of its smaller volume (approximately 1800 liters as opposed to approximately 100,000 liters in the 17-Meter Flume). The number of particles required to seed the flow in the Paddle-Wheel Flume was almost 20 times less than the number needed to achieve similar concentrations in the 17-Meter Flume.

The Paddle-Wheel Flume was 8.5 m long and 50 cm wide. Eight paddles attached to flexible linkages revolved on a large paddle wheel and drove the flow at a constant velocity. The designated "test section" where flow disturbances from the channel bend had dissipated, was located 4.2 m downstream from the first bend following the paddles, and 1.5 m (three channel widths) upstream from the downstream bend. Flow speeds were adjusted by a

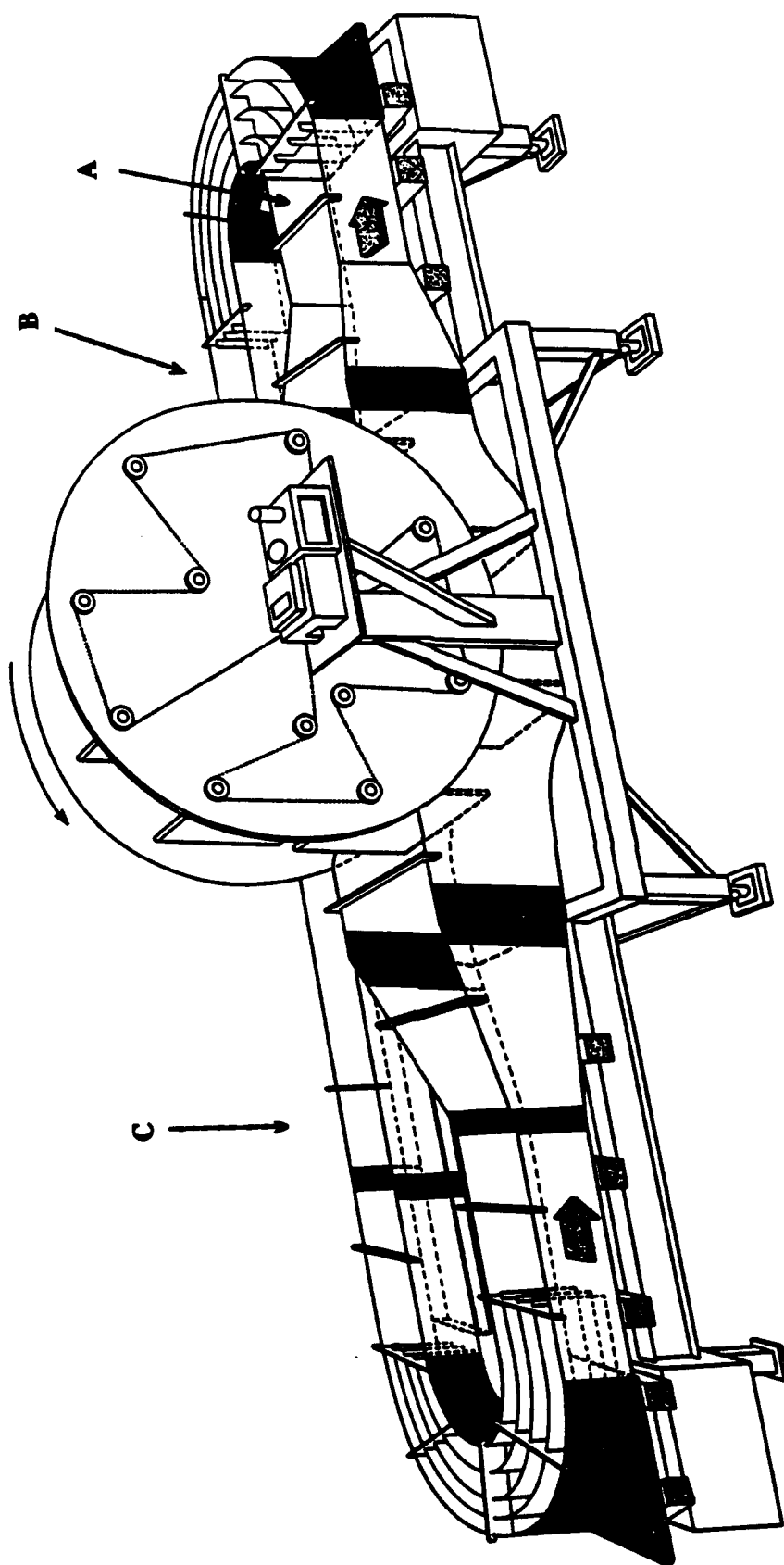


Figure 2. Schematic drawing, approximately to scale, of the Paddle Wheel flume used for the particle contact studies. Locations A, B, and C are regions where pump samples were taken to determine particle distribution in the flume. The "test section" where experimental plates were placed is located at C. Arrows represent direction of flow in the flume. Flow separators are located at both ends of the flume to reduce cross-stream flows generated while flow around bends (Figure from Butman and Grassle, submitted).



rheostat that controlled the paddle wheel motor and were verified with a Marsh McBurney electromagnetic current meter. The flume was filled to a height of 14 cm with 10  $\mu\text{m}$  filtered seawater at ambient room temperature and was allowed to warm up and deaerate overnight. This procedure was necessary because inflowing seawater at ambient winter-time temperatures was supersaturated with gasses. Deaerating the water overnight prevented bubbles that interfered with particle retention on the plates from forming during the experimental runs.

Due to the water depth in the flume (14 cm), cross-stream flow at the bottom and along the surface was expected (Butman and Grassle, submitted), but because the plates were near the center of the water column (5 cm above bottom), this cross-stream flow was not expected to quantitatively affect the outcome of this study. Furthermore, cross-stream flows should have dissipated at the test section.

Spores from the club moss *Lycopodium* sp. (Duke Scientific Company, product #215, Palo Alto, CA) were selected for use as particles in this study because of their low gravitational fall velocities and their low cost. *Lycopodium* releases pale yellow spores that, when hydrated, are 40-70  $\mu\text{m}$  in diameter. The spore density in freshwater was 1.03  $\text{g cm}^{-3}$  (Duke Scientific, pers. comm.). The fall velocities of these spores were expected to be in the range of passively sinking, deep-sea larvae and propagules, most of which are approximately 64-250  $\mu\text{m}$  in diameter (Mullineaux, unpub. data), and have predicted settling velocities of  $< 0.1 \text{ cm s}^{-1}$ .

A stock mixture of particles and seawater was made by mixing 0.25 - 0.50 g of dried spores with approximately 20 ml of 0.2  $\mu\text{m}$  filtered seawater. The mixture was shaken vigorously until most of the spores were suspended. A few drops of Betadine surgical scrub were added to relieve surface tension. The spores were then allowed to hydrate for one hour at room temperature. A small aliquot was drawn from the stock mixture, loaded into a hemacytometer, and the average number of spores per milliliter determined from the mean of six subsamples.

The flume was seeded with a known concentration of the spore-containing stock mixture. The stock mixture volume was adjusted to yield a final concentration of 75 spores per milliliter in the flume, and then was diluted to 4 liters and mixed vigorously before introduction into the flume. Spores were distributed homogeneously throughout the flume water volume by pouring the stock mixture along a full circuit of flume, in the direction opposite to the flow at 10  $\text{cm s}^{-1}$  to minimize deposition on the flume bottom. The spores were allowed to circulate two times around the flume before the rheostat was readjusted to attain the desired flow speed.

During the experimental runs, particle concentrations in the flume were measured at plate height (5 cm above the bottom). Particles were collected with a peristaltic pump sampler similar to that described by Hannan (1984). Small water samples, of known volume (150 - 250 ml), were drawn from the flume through a thin glass tube (6 mm in diameter), bent so that the intake faced directly into the flow. The tube, which was the only part of the apparatus disturbing the flow, was positioned vertically with a vernier caliper. Spores in the

pump samples were retained on a 1.2  $\mu\text{m}$  Millipore filter, and counted with a dissecting microscope. Prior to and immediately following the experimental runs, particle concentrations were measured at three heights above the bottom in three locations around the flume (locations A, B, and C in Fig. 2) to determine whether particles were well-distributed, both vertically and horizontally, throughout the flume during the course of an experimental run. No consistent trends in particle concentration, such as an increase in particles near the bottom due to settling, or near the inner, lower corners of the flume due to cross-stream flows (as described by Butman and Grassle, submitted), were observed.

The three plate treatments (faired, bluff, and split) were coated with a thin layer of Dow Corning 340 Heat Transfer Compound (DC 340), a white, viscous, silicon-based adhesive that retained particles in locations where they first contacted the plates. DC 340 was chosen over a variety of other coatings on the basis of five criteria. When applied to the plates in a thin coat, it: (1) contrasted in color with the particles; (2) formed an even, flat surface; (3) was insoluble in seawater and retained its adhesive properties over time; (4) was nontoxic for use in the flume, where live animals were frequently used, and (5) did not deform under high along-stream flows or shear stresses. Erosion experiments demonstrated that once a particle contacted a coated surface, the particle could not be dislodged even at shear stresses much higher than those occurring during experimental runs (unpub. data).

The three experimental plates, coated on their upper surfaces with adhesive, were chilled to a temperature that matched the seawater in the flume (8.5 - 12.5°C). Flume water depth averaged about 14 cm, but ranged from 13.0 to 14.5 cm; thus, the width-to-depth ratio (3.85 - 3.45 respectively) was suboptimal for one-dimensional, open-channel flow (Nowell and Jumars, 1987). Potential effects of wall boundary layers were addressed experimentally with flow visualizations and particle contact analyses. Plates were added to the flume after flow speed had been established for each experiment. Three plates were placed in the test section horizontally (side-by side, in a random order) and elevated 5 cm above the bottom on thin legs. Dye studies were conducted to determine the horizontal spacing needed to dissipate the vortices generated at the corners of the plate leading edges before they interfered with the flow over adjacent plates. The dissipation distance, of approximately 3 cm, resulted in 7 cm clearance from each flume wall. Dye studies showed that this arrangement minimized side-wall flow effects, while keeping the leading-edge flow disturbances from influencing adjacent plates.

During an individual run, three separate experiments were conducted, one at each of three flow speeds (2, 5, and 10  $\text{cm s}^{-1}$ ). In order to conserve spores, the flume was not emptied and reseeded between the three flow speed treatments; instead, between treatments, flow speed was increased to the maximum setting (approximately 20  $\text{cm s}^{-1}$ ), and a squeegee was used to resuspend particles that had settled out of suspension. Flow speed was then decreased and allowed to equilibrate to the new setting before the next set of plates was introduced. An estimate of spore concentrations during each replicate run was made by pumping water 5 cm above the bottom (plate height) at a location 4 m upstream of the test section (location B in Fig. 2). Nine pump samples were collected during each replicate run (three samples in each flow speed treatment) to determine whether particle concentration in

the flume changed significantly between subsequent flow treatments, and between replicate runs.

Particles were allowed to accumulate on the plates for 30 minutes. A fresh set of three plates was introduced at the start of each flow speed treatment. The positions of the three plate types, relative to the inner and outer walls of the flume were randomized for each flow speed treatment. In addition, the temporal order of flow treatments was randomized for the replicate runs. Flow speeds were measured at 10 cm above the bottom and verified before each flow speed treatment with a Marsh McBurney current meter. Boundary shear velocities of the flume flow were chosen to cover a range of naturally occurring deep-sea (slow) flows.

After a 30-min replicate run, plates were removed from the flume. Particle accumulation patterns within 3 cm of the leading edge of each plate were quantified by counting spores under a dissecting microscope in successive 0.5 cm bands downstream from the leading edge. Only the central 6 cm in a band were counted to avoid regions near the edge that could have been affected by secondary flows (e.g., roll vortices in Ruderich and Fernholz, 1986). Between 4.5 and 20.5 cm from the leading edge of the plates, spores were counted in 1.0 cm bands, centered at 2.5 cm intervals from the leading edge. The bands were narrower near the leading edge because strong downstream gradients in flow characteristics were expected in that region, whereas flow gradients were expected to be more gradual further downstream. Each 0.5 or 1.0 cm band was further subdivided into six 1.0 cm cells across the plate to quantify cross-stream particle distributions. Particle abundances on the plates from each flow treatment,  $P_{p(i)}$ , were adjusted to normalized values  $P'_{p(i)}$  by multiplying them by the ratio of the mean particle concentration in the flume from all replicate runs  $[\overline{P_w}]$  to the flume particle concentration during the time interval of the replicate run  $[P_{w(i)}]$ .

$$P'_{p(i)} = P_{p(i)} \cdot \overline{P_w} / [P_{w(i)}]$$

This normalization permitted comparison of particle abundances on plates between flow speeds and between replicate runs.

### 2.3 Statistical Analyses

Comparisons between particle abundances and flow characteristics were conducted with Kendall's  $\tau$  correlation coefficient (Siegel, 1956). For each plate type in the two faster flow treatments (5 and 10 cm s<sup>-1</sup>), mean particle abundances in the eight bands between 0 - 8 cm were calculated using the three replicate runs. These mean abundances were ranked for comparison with ranked values of the three flow characteristics, (vertical [plate-ward] advection, turbulence and shear stress), from comparable locations on the plates. In cases where flow measurements had not been made at the same location as particle counts, values were interpolated from the closest measurements. Similar comparisons between particle contact and flow characteristics at 2 cm s<sup>-1</sup> flow speeds were not performed because detailed flow characteristics had not been measured at this flow speed.

Additional analyses were conducted for the sole purpose of investigating possible flow biases in the experiments. Cross-stream variations in particle abundance were analyzed with a one-way ANOVA (Systat, version 2.1) on each of the 27 plates (three plates in each of three flow speed treatments in three replicate runs). The analyses were done separately for the leading edge region (0-8 cm) and the mid-plate region (10-20 cm) of each plate, to isolate effects in the developing boundary layer from those in the relatively uniform boundary layer downstream. Cross-stream variations in particle contact in the leading-edge region were of interest to evaluate the potential influences of secondary flows (e.g., roll vortices) produced at the leading edges of the plates. Cross-stream variations in the mid-plate region were expected to be less influenced by leading-edge disturbances, but were examined to determine if cross-stream flows in the flume channel influenced particle contact.

Downstream variations in particle abundance (i.e., at the leading edge versus the mid-plate regions of the 27 plates analyzed for cross-stream effects) were also analyzed separately for each plate type, using an one-way ANOVA. Replicate plates were not used as replicates in the analysis because they had been placed in a different position in the flume (i.e., inner, middle, outer) during each replicate run. Downstream particle abundances were expected to co-vary with flow gradients in the leading edge region of plates, but particle abundances were not expected to vary in the mid-plate region, where there was only moderate downstream variation in boundary-layer flow characteristics. The one-way ANOVAs tested this prediction so that particle abundances in the mid-plate region could be pooled for further analyses. Since the reliability of all above analyses depended on the assumption that particle abundances in contiguous bands on a plate were independent, the results were interpreted cautiously.

### 3 Results

#### 3.1 Flow Over Experimental Plates

Boundary-layer flows measured by the LDV over the three plate types at 5 and 10 cm s<sup>-1</sup> flow speeds (Fig. 3) corresponded to those predicted by classical boundary-layer theory and measured in open-channel flows (Kiya and Sasaki, 1983; Ruderich and Fernholz, 1986). On the faired plate, no flow separation was detected. At both 5 and 10 cm s<sup>-1</sup> flow speeds, a classical boundary layer developed, with boundary thickness increasing with distance downstream from the leading edge. Vertical advection (away from the plate) decreased downstream from the leading edge as the boundary layer grew, but did not drop below zero (i.e., where vertical advection would be toward the plate). Turbulence and shear stress tended to be elevated slightly at the leading edge where the boundary layer was thin and a slight bow wave may have existed. The exception was shear stress at the leading edge in the 5 cm s<sup>-1</sup> flow, which was lower than over the rest of the plate. This anomalous result may have been due to the measurement being taken slightly above the boundary layer, rather than within it (Mullineaux and Butman, 1991). Further downstream, turbulence and shear stress decreased to lower, relatively constant values. Turbulence and shear stress tended to be higher in 10 cm s<sup>-1</sup> than in 5 cm s<sup>-1</sup> along-stream flow speeds, and were higher over the bluff and split plates

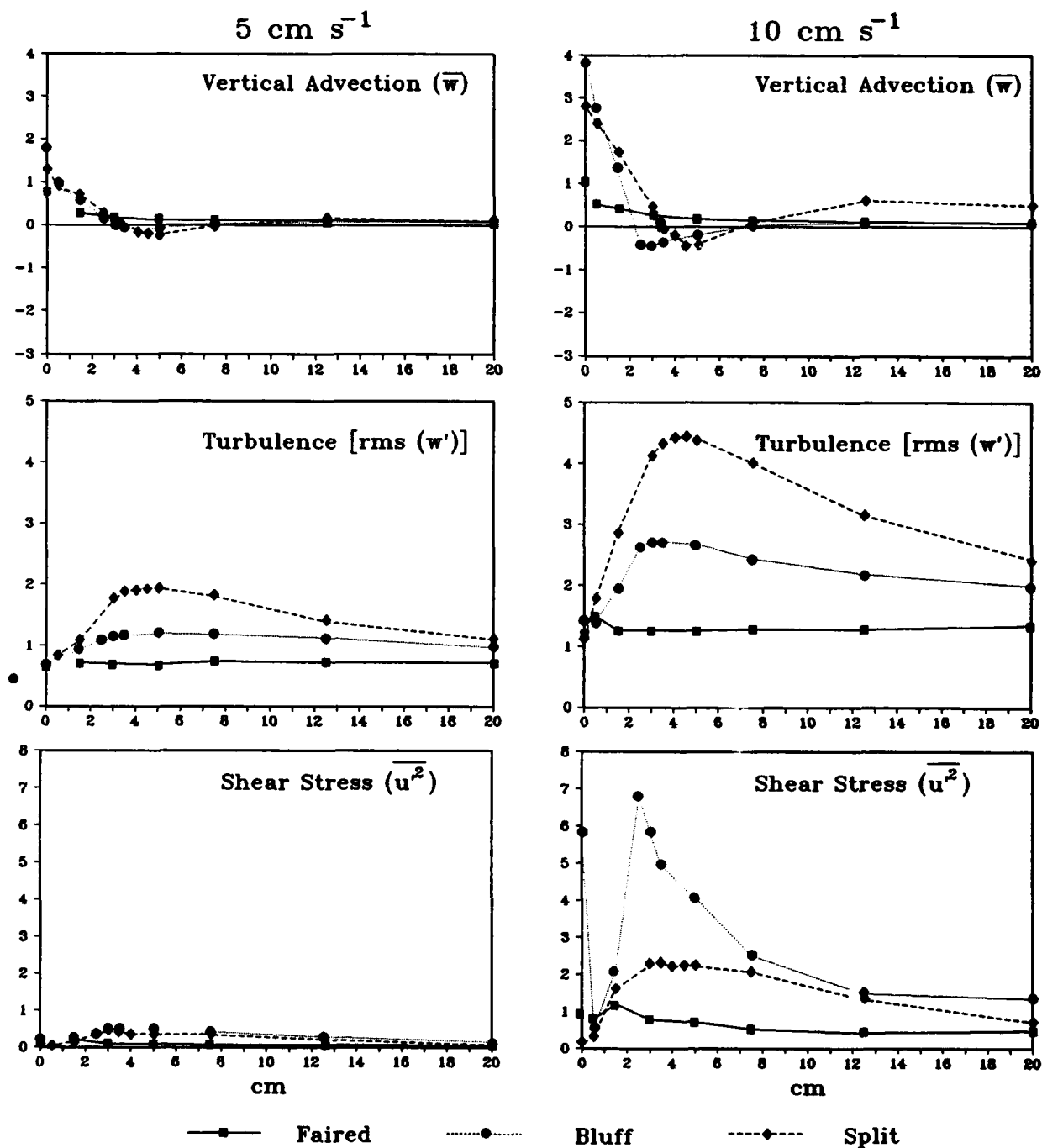


Figure 3. Boundary-layer flow characteristics calculated from 2-axis laser Doppler velocimeter measurements. Mean fluctuating flows were measured over faired, bluff, and split plates at along-stream velocities of 5 and 10 cm s<sup>-1</sup> measured at 10 cm above flume bottom. Vertical (normal to the plate) advection ( $\bar{w}$ ) and turbulence [rms( $w'$ )] were integrated over vertical profiles between 0.2 and 2.0 cm above the plate surface. Boundary shear stress ( $\overline{u'^2}$ ) was measured at 0.1 cm above each plate. Data symbols not connected by lines represent suspect measurements (see Results).

than over the faired plate.

The highest shear stresses occurred on the bluff plates in a region extending from 1-5 cm downstream of the leading edge; these were substantially higher than those over a similar region on the split plates. Reduced shear stress on the split plate, downstream of the splitter bar, was likely due to protection of the plate from incident flows. These patterns were intensified at the higher along-stream flow speed. Both turbulence and shear stress values decreased to a moderate, but constant level in the mid-plate regions of the split and bluff plates, although the values were consistently higher than over the faired plates.

Vertical advection away from the plate was high at the leading edge of both the bluff and split plates where flow separations formed, but decreased sharply (i.e., vertical advection toward the plate increased) as the flow reattached to the plates, 2 to 5 cm downstream. The reattachment position on both plates varied with changes in along-stream flow speeds. On the bluff plate at  $5 \text{ cm s}^{-1}$ , flow reattached 4.5 - 5.0 cm downstream from the leading edge, but at  $10 \text{ cm s}^{-1}$  the reattachment point was located between 3.5 and 4.5 cm downstream. Generally, the reattachment point on the bluff plates was located between 0.5 and 1.0 cm upstream from the reattachment point on the split plates in comparable along-stream flow speeds. Dye studies indicated that the downstream extent of the separation eddy increased with increasing flow speed up to a critical speed, where the separation eddy became unstable. The observation that reattachment in  $10 \text{ cm s}^{-1}$  flow was closer to the leading edge than in  $5 \text{ cm s}^{-1}$  flow suggested that at  $10 \text{ cm s}^{-1}$  the separation eddies became unsteady and appeared smaller because they were being shed more frequently (as in Ruderich and Fernholz, 1986). The reattachment point corresponded with the region of highest shear stress on both the split and bluff plates.

Flow visualizations with dye on bluff and faired plates corroborated the LDV measurements at higher flow speeds, and contributed insight into behavior of boundary-layer flows over plates in  $2 \text{ cm s}^{-1}$  along-stream flows. Dye injected along the leading edge of a bluff plate followed the contour of the plate in along-stream flows of  $2.0 - 2.8 \text{ cm s}^{-1}$ , outlining a boundary layer qualitatively similar to that over a faired plate, but with a higher boundary-layer growth rate. Visualizations at along-stream flow speeds between 5 and  $13 \text{ cm s}^{-1}$  indicated that a separation eddy formed and grew in height and length with increasing flow speed up to  $9 \text{ cm s}^{-1}$ . Separation eddies in faster flow speeds were unstable and were shed frequently.

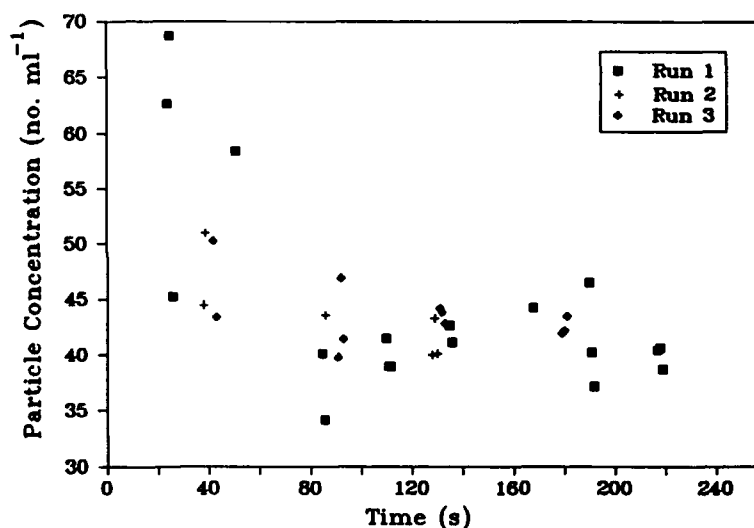
Downstream flow variations were most pronounced in the region 0-8 cm from the leading edge of all three plate types, where the boundary layer was developing and flow separations occurred. Flow disturbances produced at the leading edge dissipated downstream, and the boundary layer at distances greater than 10 cm from the leading edge grew so slowly that a change in boundary-layer thickness was not noticeable on regions downstream from this point. Because of this qualitative difference, downstream variations in particle contact on the "leading edge" region only were compared to downstream variations in vertical (plate-ward) advection, turbulence and shear stress. In contrast, particle abundances on the "mid-plate" region (10-20 cm) were pooled and analyzed relative to along-stream flow speeds and particle

fluxes. The flow in this region was considered "non-varying", although the boundary layer was still developing slightly.

### 3.2 Particle Concentrations in the Flume

Preliminary measurements indicated that particles were well-distributed throughout the flume during experimental runs, so subsequent particle concentration measurements were taken at plate height in the section of the flume where the plates were placed. Particle concentrations in the flume were consistent between replicate runs and, with the exception of the first run, decreased only slightly (4.7 to 11.1 %) over the course of the three flow treatments (speed adjustments) within each run (Fig. 4). Mean particle concentrations, measured during each flow treatment (Table 1), were used to adjust corresponding particle abundance on the plates, so they could be compared between flow speeds and between replicates. All plate abundances were normalized to a mean flume particle concentration of  $44.50 \text{ ml}^{-1}$ .

**Figure 4.** Particle concentrations in the flume during three replicate runs determined by counting number of spores per ml from pump samples drawn from Location B (Fig. 2). Mean numbers collected during each of the three flow speed treatments in each replicate run were used to normalize particle abundances on plates (Table 1).



### 3.3 Particle Contact Patterns

Particle accumulation on the plates in the leading edge regions was used as a measure of particle contact, since previous experiments had shown that erosion was negligible. Particle contact, normalized by particle concentration in the flume, varied downstream from the leading edge of all plates, and also varied slightly between plate types and flow speeds (Fig. 5).

Particle contact on the faired plate showed a strong pattern relative to the leading edge at all three flow speeds, with contact increasing with distance downstream in the leading edge region and becoming relatively constant in the mid-plate region (Fig. 5a). Contact near the

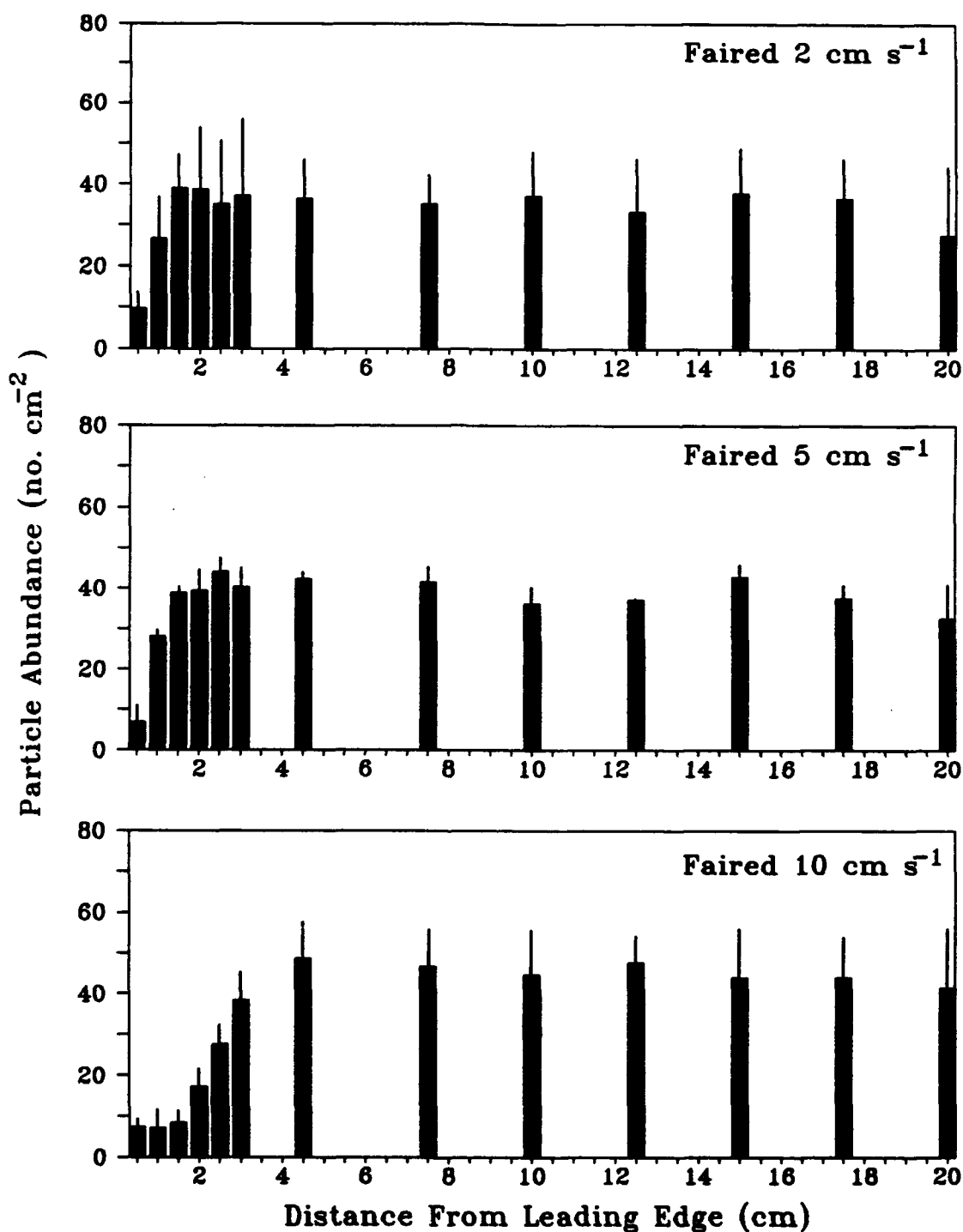
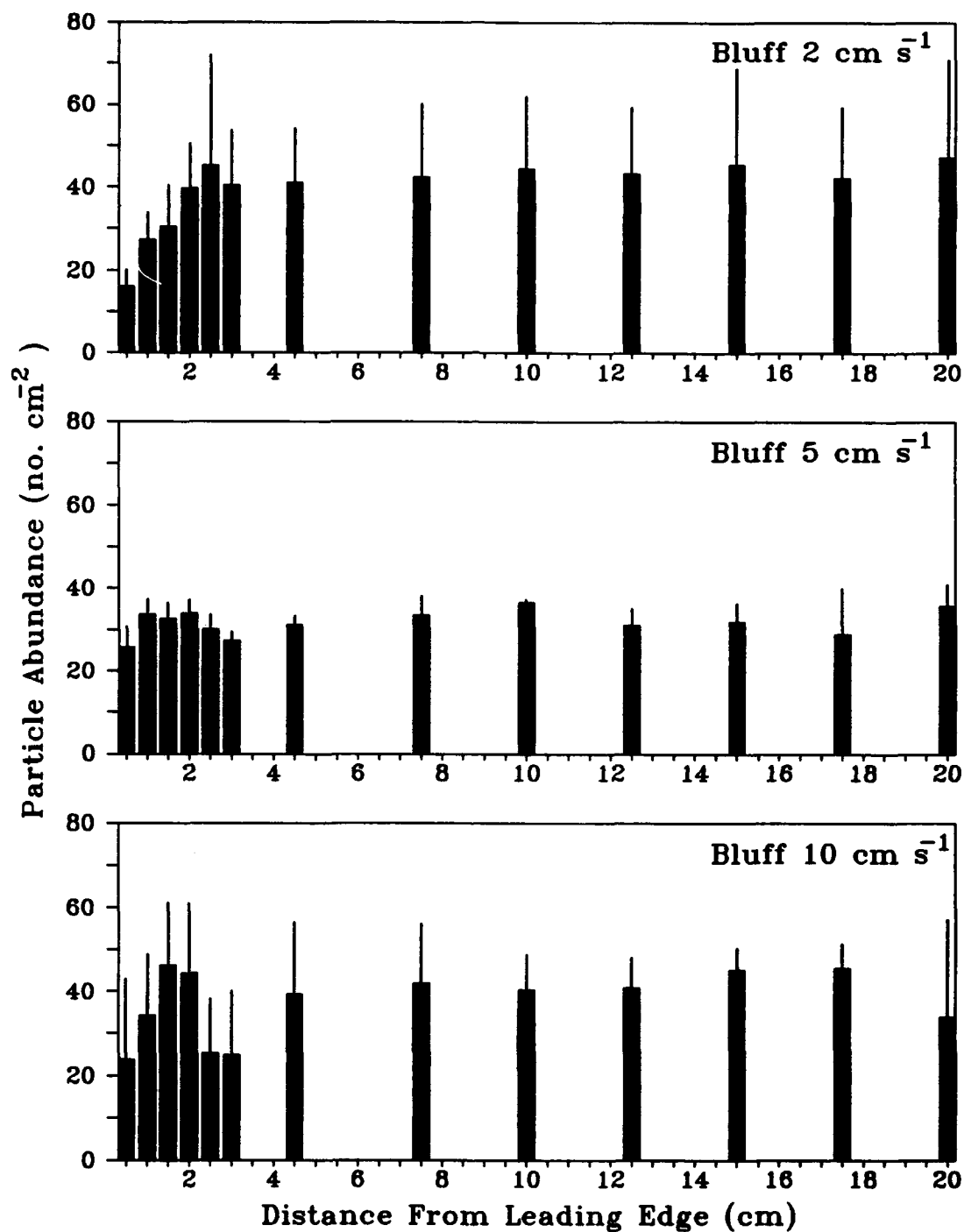
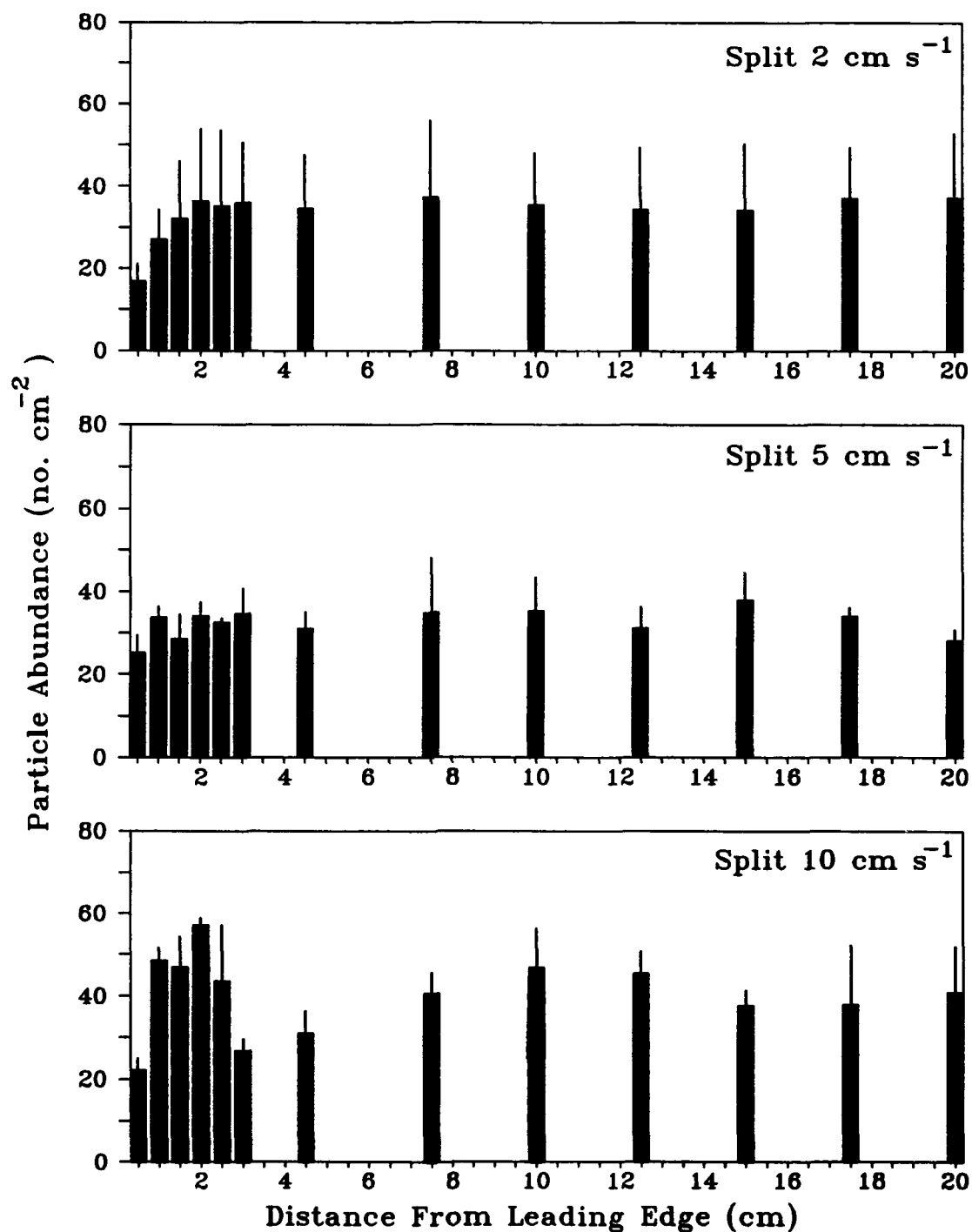


Figure 5a. Particle distribution (normalized by flume particle concentration) on faired plates at flume flow speeds of 2, 5, and 10 cm s<sup>-1</sup>. Means and standard deviations are shown from three replicate flume runs. Values from 0-3 cm represent abundances in 0.5 cm intervals; values from 5-20 cm represent abundances in 1.0 cm intervals, centered at the marked distance.





**Figure 5b.** Particle distribution (normalized by flume particle concentration) on bluff plates at flume flow speeds of 2, 5, and 10 cm s<sup>-1</sup>. Means and standard deviations are shown from three replicate flume runs. Values from 0-3 cm represent abundances in 0.5 cm intervals; values from 5-20 cm represent abundances in 1.0 cm intervals, centered at the marked distance.



**Figure 5c.** Particle distribution (normalized by flume particle concentration) on split plates at flume flow speeds of 2, 5, and 10 cm s<sup>-1</sup>. Means and standard deviations are shown from three replicate flume runs. Values from 0-3 cm represent abundances in 0.5 cm intervals; values from 5-20 cm represent abundances in 1.0 cm intervals, centered at the marked distance.

leading edge of plates in  $2 \text{ cm s}^{-1}$  and  $5 \text{ cm s}^{-1}$  flows was reduced only in the 0-1 cm bands, whereas contact on the plates in  $10 \text{ cm s}^{-1}$  flows was reduced throughout the 0-3 cm bands. Because the flow characteristics of turbulence, vertical advection and shear stress all decreased with distance from the leading edge at  $5 \text{ cm s}^{-1}$  and  $10 \text{ cm s}^{-1}$ , contact was negatively correlated (Kendall's  $\tau$  correlation coefficient,  $p < 0.05$ ) with all three flow characteristics (Table 2).

Flume Flow Speed	$2 \text{ cm s}^{-1}$ (no. $\text{ml}^{-1}$ )	$5 \text{ cm s}^{-1}$ (no. $\text{ml}^{-1}$ )	$10 \text{ cm s}^{-1}$ (no. $\text{ml}^{-1}$ )
Replicate #1	38.69	42.65	58.71
Replicate #2	41.13	41.77	46.20
Replicate #3	42.51	45.19	43.61

**Table 1.** Mean particle concentrations the flume for each flow speed treatment during each of three replicate runs. Means were calculated from particle concentrations measured in at least three pump samples (Fig. 4), except for Replicate #2 at  $5 \text{ cm s}^{-1}$  ( $n=2$ ). These means were used to normalize particle contact data to a standard flume concentration of particles (arbitrarily chosen to be the grand mean of  $44.50 \text{ particles ml}^{-1}$ ).

Plate Treatment and Flow Speed	Vertical Advection	Turbulence	Shear Stress
Faired			
$5 \text{ cm s}^{-1}$	-0.714 *	-0.643 *	-0.714 *
$10 \text{ cm s}^{-1}$	-0.857 *	-1.000 *	-0.857 *
Bluff			
$5 \text{ cm s}^{-1}$	0.000	0.071	-0.214
$10 \text{ cm s}^{-1}$	0.143	-0.143	-0.500 *
Split			
$5 \text{ cm s}^{-1}$	-0.500 *	0.429	0.429
$10 \text{ cm s}^{-1}$	0.214	-0.286	-0.214

\*  $P < 0.05$

**Table 2.** Nonparametric correlation (Kendall's  $\tau$ ) between positions of particle contact and flow characteristics on three-plate treatments. Values ranked from eight positions downstream from the leading edge. Particle contact ranks were assigned to the average of three replicate runs at each flow speed. Ranks for the flow characteristics were assigned to mean values from 4-min sampling intervals.

Contact on the leading edge of the bluff plates appeared to peak between 1-2 cm downstream of the leading edge at 5 and 10 cm s<sup>-1</sup> flow speeds (Fig. 5b). The absence of this peak at 2 cm s<sup>-1</sup> flows, where no flow separation was observed, suggested that enhanced contact in the faster flows was a consequence of the flow separation. The effect of the separation on contact was much more prominent at 10 cm s<sup>-1</sup> than at 5 cm s<sup>-1</sup>. Contact patterns on bluff plates in 5 cm s<sup>-1</sup> flows were difficult to interpret because variations in the mid-plate region were as great or greater than variations near the leading edge.

No correlation was found between contact and vertical advection on the bluff plates at 5 or 10 cm s<sup>-1</sup> flow speeds. Although contact was consistently low at the leading edges, where vertical advection was directed away from the plate, it was also low at the reattachment point, where vertical flows were towards the plate. No consistent correlation was found between contact and turbulence at 5 and 10 cm s<sup>-1</sup>, or between contact and shear stress at 5 cm s<sup>-1</sup>; the peaks in turbulence and shear stress intensities tended to be located further downstream than the peaks in contact. The shear stress maximum at 10 cm s<sup>-1</sup> corresponded in location to the contact minimum, resulting in a significant negative correlation.

Contact patterns over the bluff plates at 2 cm s<sup>-1</sup> were similar to those over the faired plates at 2 cm s<sup>-1</sup>. Since no separation over the bluff plate was observed at 2 cm s<sup>-1</sup>, it is likely that boundary-layer development was similar to that over the faired plate. The similarity in flows may account for the similarity in contact patterns between the two plate types.

Particle contact on the split plates was low at the leading edge in all flows, and increased with distance downstream in the 2 and 5 cm s<sup>-1</sup> flow speeds (Fig. 5c). In 10 cm s<sup>-1</sup> flows, contact peaked under the separation eddy and decreased at the reattachment point. No consistent correlations between contact and flow characteristics were observed, and the only significant correlation was with vertical advection at 5 cm s<sup>-1</sup>. This correlation reflected a slight increase in contact with distance from the leading edge in the 0-3 cm region, where vertical advection was decreasing.

Downstream patterns of particle abundance, and their correlations with flow patterns were of primary interest in this study, but cross-stream patterns were also quantified. These cross-stream analyses were used only to test the assumptions that flow disturbances generated at the edges of plates did not influence particle contact on neighboring plates, and that cross-channel flows in the flume did not influence particle accumulation patterns.

Only three of the plates showed significant variation in cross-stream particle abundances in the leading edge region (Table 3). The three plates included a bluff plate in 5 cm s<sup>-1</sup> flow positioned near the inner wall of the flume, another bluff plate in 5 cm s<sup>-1</sup> flow positioned in the center of the flume, and a split plate in 2 cm s<sup>-1</sup> flow positioned near the inner wall. Consistent trends in particle contact in the cross-stream direction did not occur for any plate type at any flow speed. Visual inspections of these graphed data (not shown) also revealed no consistent trends of increased or decreased particle abundances along the

edges of plates adjacent to other plates. These results suggest that secondary flows produced at a plate leading edge did not influence particle contact on adjacent plates. The graphs also revealed no consistent increase in particle abundance from the outer to inner sides of a plate, as would be expected if cross-channel flume flows were accumulating particles along the inner walls (as in Butman and Grassle, submitted). Six different plates showed significant cross-stream variation in the mid-plate region but visual inspection of these data again revealed no consistent trends.

Plate	Position	2 cm s <sup>-1</sup>		5 cm s <sup>-1</sup>		10 cm s <sup>-1</sup>	
Treatment		Lead	Mid	Lead	Mid	Lead	Mid
<b>Faired</b>							
Run 1	Middle	0.11	1.11	0.46	0.55	0.04	1.55
Run 2	Inner	0.54	0.19	0.63	2.73 *	0.18	0.36
Run 3	Outer	0.64	0.12	0.17	0.41	0.26	2.27
<b>Bluff</b>							
Run 1	Inner	1.17	2.78 *	2.72 *	1.28	1.24	2.65 *
Run 2	Outer	0.02	1.54	2.21	1.12	0.82	1.28
Run 3	Middle	1.00	0.68	2.54 *	0.91	0.42	0.08
<b>Split</b>							
Run 1	Outer	0.22	1.10	0.67	1.38	0.94	3.02 *
Run 2	Middle	0.69	1.84	2.07	2.82 *	0.97	0.28
Run 3	Inner	6.06 †	0.05	0.72	2.86 *	0.75	0.05

\* P < 0.05                      † P < 0.01

**Table 3.** F ratios from ANOVA of cross-stream particle abundances on the plates in the region 0-8 cm downstream of the leading edge (Lead), and the region 10-20 cm downstream (Mid). The particles in six 1-cm by 0.5-cm cells were counted from eight 0.5-cm-deep bands oriented perpendicular to the flow in the leading edge region (Lead; df=5, n=8), and the particles in six 1-cm by 1-cm cells were counted from five 1-cm-deep bands further downstream (Mid; df=5, n=5).

Downstream particle abundances were analyzed with parametric statistics (ANOVA) to determine whether variations in particle contact in the mid-plate region were small relative to those in the leading edge region. Near the leading edge, significant downstream variations ( $P < 0.05$ ) were found on 23 of the 27 plates (Table 4), whereas further downstream, significant variations were found on only eight of the plates. Visual inspection of the patterns on these eight plates revealed no consistent trends in particle contact related to distance from the leading edge. The eight plates showing significant variation included all plate types (three faired, two bluff and three split), flow speeds (two at 2 cm s<sup>-1</sup>, three at 5 cm s<sup>-1</sup>, and three at 10 cm s<sup>-1</sup>) and positions in the flume (three near inner wall, three in the middle, and two near the outer wall). These results suggest that downstream variations in particle contact on the mid-plate regions may have been independent of any of the measured flow characteristics.

Plate	Position	2 cm s <sup>-1</sup>		5 cm s <sup>-1</sup>		10 cm s <sup>-1</sup>	
Treatment		Lead	Mid	Lead	Mid	Lead	Mid
<b>Faired</b>							
Run 1	Middle	11.36 †	0.77	13.78 †	3.33 *	28.55 †	3.21 *
Run 2	Inner	9.64 †	2.09	11.34 †	1.65	59.99 †	2.01
Run 3	Outer	4.04 †	17.48 †	20.70 †	1.79	23.93 †	2.71
<b>Bluff</b>							
Run 1	Inner	7.19 †	1.63	1.01	9.20 †	5.67 †	1.45
Run 2	Outer	13.81 †	0.69	0.87	1.13	4.43 †	0.07
Run 3	Middle	2.76 *	0.11	1.17	0.71	14.40 †	10.35 †
<b>Split</b>							
Run 1	Outer	10.62 †	0.58	2.61 *	3.57 *	10.10 †	0.66
Run 2	Middle	2.91 *	1.98	2.27 *	0.69	9.24 †	2.34
Run 3	Inner	1.43	5.00 †	2.64 *	0.82	8.70 †	5.00 †
		* P < 0.05		† P < 0.01			

**Table 4.** F ratios from ANOVA of downstream particle abundances on the plates in the region 0-8 cm downstream of the leading edge (Lead), and the region 10-20 cm downstream (Mid). The particles in eight 0.5-cm by 1-cm cells were counted from six 1-cm-wide strips running parallel to the flow in the leading edge region (Lead; df=7, n=6), and particles in five 1-cm by 1-cm cells were counted in the six 1-cm-wide strips further downstream (Mid; df=4, n=6).

### 3.4 Particle Contact Rates

Particle abundance was measured away from the effects of the plate leading edges (10 - 20 cm downstream) to calculate contact rates in non-varying boundary-layer flows. The absence of flow-related variations in particle contact in this mid-plate region (Table 4) indicated that these particle contact data could be pooled for subsequent analyses. Mean contact rates were then compared between plate types and between along-stream flow speeds.

Particle contact rates on the mid-plate region varied strongly with along-stream particle flux (Fig. 6). Contact rates did not, however, vary strongly with along-stream flow speed (Fig. 7). A two-way ANOVA revealed no significant ( $P < 0.05$ ) variation with either flow speed or plate type in the "non-varying" flow region of the plates. Thus, the observed increase in particle contact rate on plates in increasing along-stream particle fluxes appears to have been due almost entirely to increases in particle concentration in the flume.

**Figure 6.** Particle contact rate on mid-plate region as a function of along-stream flux (calculated from the product of particle concentration in the flume and along-stream flow speed). Contact rate is expressed as number of particles (not normalized) accumulating on five 1-cm bands in the region 10-20 cm downstream from the leading edge during a 30-min interval.

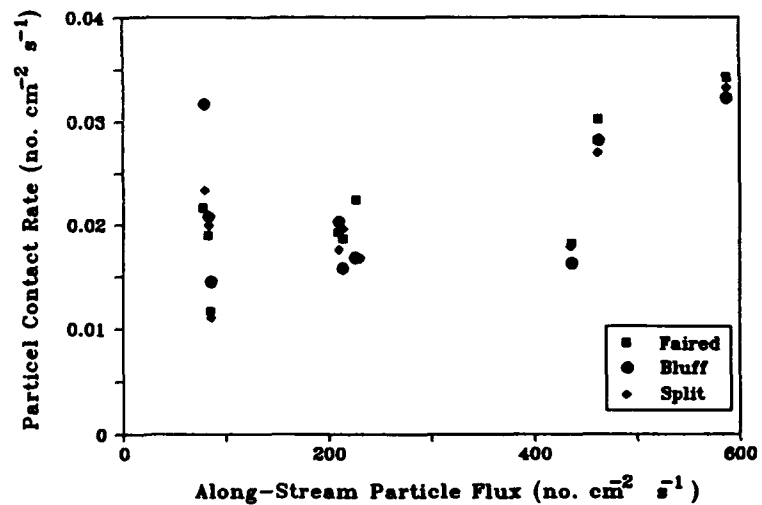
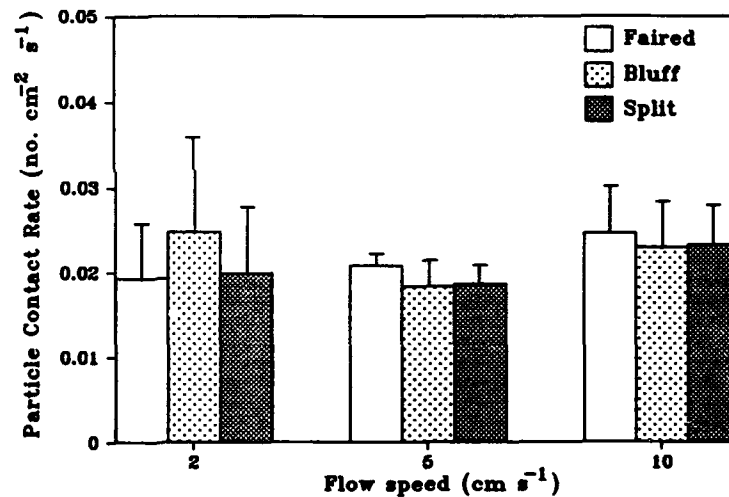


**Figure 7.** Particle contact rates (normalized) on the experimental plates. Values plotted are mean (and standard deviation) of contact rates for three replicate runs.



## 4 Discussion

### 4.1 Particle Contact Patterns in a Developing Boundary Layer

The lack of consistent correspondence between particle contact patterns on the leading edge region of plates and individual flow characteristics (vertical [plate-ward] advection, turbulence, shear stress) suggests that several aspects of the flow are interacting to produce

the observed particle patterns. We had predicted that increasing plate-ward advection and turbulence in the boundary layer would increase particle contact by increasing the flux of particles through the boundary layer (as in Eckman, 1990). A significantly positive relationship between particle contact and plate-ward advection or turbulence was not observed, however, on any of the plates. One explanation for this unanticipated result is that elevated values of plate-ward advection and turbulence are often associated with enhanced shear stress very near the plate (Fig. 3), which may inhibit the particles from settling (Eckman, 1990). It is important to note that effects of shear stress are acting on particle motions in the water column, and are not causing particle erosion. No evidence of post-contact particle motion or erosion (e.g., pits or trails in the adhesive) were observed on the plates.

A closer examination of particle patterns within plate types reveals that high particle contact rates occurred only in regions with both a relatively thick boundary layer and reduced shear stress. Regions with only a thick boundary layer (e.g., the reattachment points on the bluff and split plates) or reduced shear stress (within 0.5 cm of the leading edge of bluff and split plates) did not collect particles, hence the non-significant correlations with particle contact on these plates (Table 2). We suggest that mixing in the thicker boundary layer downstream from the plate leading edges enhances the flux of particles from the water column into the boundary layer, but once in the boundary layer, particle contact is enhanced only in regions with low shear stress. Plate-ward advection may also increase the flux of particles into the boundary layer, although particle contact does not appear to be enhanced at reattachment points due to elevated shear stresses.

#### 4.2 Implications for Larval Settlement in a Developing Boundary Layer

Results of these particle contact experiments can be applied to models of larval settlement, but only if a hydrodynamic similarity between particles and sinking larvae exists. Near bottom shear stress will only inhibit particle (or larval) contact if the ratio of particle settling velocity to shear velocity (a correlate of shear stress) is low (Eckman, 1990). In the present study, the particles used had a low specific gravity and low settling velocities. Assumptions were made that (1) particles followed streamlines, (2) particle-particle interactions were negligible, and (3) particle settling velocities were small relative to turbulent intensities and shear velocities. No evidence of particle clumping was observed, and the results suggested that gravitational and inertial forces were less important than boundary-layer motions, except very near the plate. These same assumptions are probably valid for small larvae, such as many of those in the deep sea, but are not likely to be valid for large larvae such as barnacle cyprids.

Evidence that swimming speeds, inertia or settling velocity of a larva may be important in boundary-layer flows can be found in settlement data for barnacles in controlled flume flows. In a series of experiments quantifying cyprid contact, exploration and settlement on plates in flows identical to those used in this particle study, initial cyprid contact was found to be highest at the reattachment points on the bluff and split plates (Mullineaux and Butman, 1991). This result suggests that cyprid settling velocities or swimming speeds are



sufficiently large to overcome the turbulence and shear stress at the flow reattachment points.

Small particles with low settling velocities are expected to contact vertical plates in patterns similar to those observed on horizontal plates because the boundary-layer pressure and turbulence parameters are equivalent. This assumption was not tested in the flume experiments presented here because the vertical plates were not easily elevated above the strongly sheared flows near the bottom of the flume. High settling velocities of large larvae, however, may cause them to contact upper surfaces of horizontal plates more frequently and in different patterns than they contact vertical plates. Thus, it may be important to test contact patterns of large particles on both horizontal and vertical surfaces.

An additional caveat for the use of particle contact patterns in larval settlement studies is that they are intended to predict initial contact patterns, which are not always maintained in subsequent settlement patterns. Especially in shallow-water habitats, where larvae may be relatively large and have diverse behaviors, post-contact larval behaviors may substantially influence settlement patterns. Although some of these behaviors are flow-dependent (e.g., Crisp 1955; Mullineaux and Butman, 1991), they are not well documented for most larvae. Thus it seems reasonable to caution that behavior (ie. swimming, phototaxis, chemotaxis, geotaxis, rheotaxis, etc.) and hydrodynamic character of the larva (related to size, density and shape) may significantly influence larval settlement in the field.

#### 4.3 Particle Contact Rates in the Non-Varying Flow Region

Particle fluxes to the mid-plate region (downstream of the developing boundary layer) varied only slightly (and not significantly) with along-stream flow speed. Our initial expectation was that particle flux would increase with increasing flow speed, as a result of increased turbulent mixing of particles through the boundary layer toward the surface. The absence of an increase in particle contact with increasing flow speed corroborates our observations, from developing boundary layers, that enhanced turbulence does not necessarily increase particle contact. It is likely that, in both the developing boundary layer and the non-varying flow region, particle contact depends on the relative values of particle settling velocity, integrated turbulence through the boundary layer and boundary shear stress. Over the range of flows used in this experiment ( $2\text{--}10\text{ cm s}^{-1}$ ), these factors appear to balance each other in such a way as to maintain a relatively constant contact rate, independent of along-stream flow speed. Rather than depending on flow speed, particle contact appears to depend most strongly on particle abundance in the water column.

The empirical results from this study can be used to predict the flux of particles to a plate,  $F_p$ , from particle concentration in the water  $[P_w]$  in the range of flow speeds tested:

$$(2) \quad F_p = F_w \cdot R(u) ;$$

where  $F_p = P_p/t$  (the particle accumulation over time in  $\text{cm}^{-2}\text{ s}^{-1}$ ),  $u$  is the along-stream flow speed ( $\text{cm s}^{-1}$ ),  $F_w = [P]_w \cdot u$  (the along-stream flux of particles in the water in  $\text{cm}^{-2}\text{ s}^{-1}$ ) and  $R(u)$  is the empirically measured ratio of  $F_p/F_w$  at each flow speed. Since values of

particle contact did not vary with along-stream flow speeds in the range of flows used in these experiments, this equation can be simplified to:

$$(3) \quad F_p = [P_w] \cdot K ;$$

where  $K$  (in  $\text{cm s}^{-1}$ ) is the empirically determined value of particle contact rate divided by particle concentration in the flume (normalized values plotted in Fig. 7). The mean value of  $K$  from three replicates of each plate type in three flow speeds was  $4.79 \cdot 10^{-4} \text{ cm s}^{-1}$  (st. dev. =  $1.23 \cdot 10^{-4} \text{ cm s}^{-1}$ ). The variation in these measurements was relatively high between replicate plate types within each flow speed, but was relatively low between plate types and flow speeds. This result suggests that estimates of particle concentration in the water column should not be calculated from only a few replicate plates. In addition, estimates from the simplified equation (3) are valid only in flows similar to those used in the flume ( $2 - 10 \text{ cm s}^{-1}$ ), and for regions of the plate in non-varying boundary layer flow.

#### 4.4 Interpreting Larval Settlement Plates

Predicting particle concentrations in the water from particle contact rates on flat plates may be useful in interpreting larval abundances on settlement plates. Quantification of larval abundances in the open ocean can be very difficult, especially in deep-sea habitats where traditional ship-board sampling methods (net tows) are difficult to use, and larvae are relatively sparse. Measuring larval abundances by quantifying their settlement onto artificial surfaces suspended in the water column is an attractive alternative to net tows because larval abundances can be integrated over a period of time, and only benthic larvae (and not large volumes of holoplankton and flocculent material) are collected. The limitation of this technique is that the relationship between larval settlement rates and larval abundances is influenced by often-unmeasured factors including larval contact rate with the plate and active larval behaviors. Contact rates of small larvae with the plate are expected to be controlled by the same processes controlling contact rates of small particles, but larval settlement rates will differ because not all larvae will choose to settle on contact. This behavior can be parameterized as a "choice" term,  $C_{(larva)}$ , representing the probability of larval settlement on contact. This choice term can be integrated into the particle contact equation to formulate a larval settlement equation:

$$(4) \quad S_p = F_w \cdot R_{(u)} \cdot C_{(larva)} ;$$

where  $S_p$  is the larval settlement rate onto the plate ( $\text{cm}^{-2} \text{ s}^{-1}$ ), and  $F_w$  is the along-stream flux of larvae past the plate ( $\text{cm}^{-2} \text{ s}^{-1}$ ).

In relatively slow flows, similar to those in many deep-water habitats, the larval choice term can be used with the simplified version of the particle contact equation (3), resulting in a simplified larval settlement equation:

$$(5) \quad S_p = [L_w] \cdot K \cdot C_{(larva)} ;$$

where  $[L_w]$  is the concentration of larvae in the water column ( $\text{cm}^{-3}$ ).

In deep-water habitats, larval behavioral responses at settlement are probably species-specific, and may depend on a combination of surface cues and environmental factors, including flow speed. Even in flow regimes where larval contact rates may not be strongly flow-dependent, it is possible that larval behavioral responses are. Most of these active larval responses are unknown, but they are not likely to vary between settlement plates deployed in deep-water habitats characterized by weak gradients in light, temperature, and current speeds. Thus, relative differences in larval settlement between plates in these types of habitats can be used to estimate relative differences in larval abundances. Since larval settlement responses may be flow dependent, however, unexpected variability may be introduced into settlement onto plates in different flows, even in the range of flow speeds where larval contact is independent of speed.

Interpretation of larval settlement rates in terms of larval abundances should be done cautiously, but if the settlement plates are oriented parallel to the flow, and the flow rates are measured, then relative differences in larval settlement on the plates should reflect relative differences in larval abundances in the water column.

## 5 Acknowledgements

Much of the approach, experimental design, and analysis for this project came from many discussions with Cheryl Ann Butman, John Trowbridge, and Rocky Geyer. Funding for the study was provided by the Office of Naval Research under Grant Number N00014-89-1341 to L.S.M and Grant Number N00014-89-J-1112 to C.A. Butman and L.S.M.. The Coastal Research Center at WHOI provided funds for the flume research.

## 6 Literature Cited

- Agrawal, Y.C. and C.H. Belting. 1988. Laser velocimetry for benthic sediment transport. *Deep-Sea Res.* 35: 1047-1067.
- Butman, C.A. 1986. Larval settlement of soft-sediment invertebrates: some predictions based on analysis of near-bottom velocity profiles. In: J.C.J Nihoul (ed.). *Marine Interfaces Ecohydrodynamics*. Elsevier Oceanogr. Ser., Vol. 42, Elsevier. Amsterdam, pp 487 - 513.
- Butman, C.A. 1987. Larval settlement of soft-sediment invertebrates: the spatial scales of pattern explained by active habitat selection and the emerging role of hydrodynamical processes. *Oceanogr. Mar. Biol. Annu. Rev.* 25: 113-165.
- Butman, C.A., and R.J. Chapman. 1989. The 17-Meter Flume at the Coastal Research Laboratory. Part I: Description and user's manual. WHOI Tech. Rep. 89-10. 31 p.

- Butman, C.A. and J.P. Grassle. Submitted. Active habitat selection by *Capitella* sp. I larvae: I. Simple two-choice experiments in still water and flume flows. (Submitted to J. Mar. Res. 1992).
- Crisp, D.J. 1955. The behavior of barnacle cyprids in relation to water movement over a surface. J. Exp. Biol. 32:569-590.
- Duggins, D.O., J.E. Eckman, and A.T. Sewell. 1990. Ecology of understory kelp environments. II. Effects of kelps on recruitment of benthic invertebrates. J. Exp. Mar. Biol. Ecol. 143: 27-45.
- Eckman, J.E. 1990. A model of passive settlement by planktonic larvae onto bottoms of differing roughness. Limnol. Oceanogr. 35(4): 887-901.
- Hannan, C.A. 1984. Initial settlement of marine invertebrate larvae: The role of passive sinking in a near-bottom turbulent flow environment. Ph.D. thesis, Woods Hole Oceanogr. Inst./Mass. Inst. Technol. Joint Program. 534 p.
- Keen, S.L. 1987. Recruitment of *Aurelia aurita* (Cnidaria: Scyphozoa) larvae is position-dependent, and independent of conspecific density, within a settling surface. Mar. Ecol. Prog. Ser. 83: 151-160.
- Kiya, M. and K. Sasaki. 1983. Structure of a turbulent separation bubble. J. Fluid Mech., 137, 83-113.
- Middleton, G.V., and J.B. Southard. 1984. Mechanics of sediment movement. Society Economic Paleontologists and Mineralogists, Vol. 2. Tulsa, Oklahoma.
- Mullineaux, L. S. 1992. Implications of mesoscale flows for dispersal and retention of larvae in deep-sea habitats. In: K. J. Eckelbarger and C. M. Young, eds. "Reproduction, Larval Biology and Recruitment in the Deep-Sea Benthos". Columbia University Press (in review).
- Mullineaux, L.S. and C.A. Butman, 1990. Recruitment of benthic invertebrates in boundary-layer flows: a deep water experiment on Cross Seamount. Limnol. Oceanogr. 32: 409-423.
- Mullineaux, L.S. and C.A. Butman. 1991. Initial contact, exploration and attachment of barnacle (*Balanus amphitrite*) cyprids settling in flow. Mar. Biol. 110: 93-103.
- Nowell, A.R.M. 1983. The benthic boundary layer and sediment transport. Rev. Geophys. Space Phys. 21: 1181-1192.
- Nowell, A.R.M. and P.A. Jumars. 1987. Flumes: Theoretical and experimental considerations for simulation of benthic environments. Oceanogr. Mar. Biol. Ann. Rev. 25: 91-112.

- Paola, C. 1983. Flow and skin friction over natural rough beds. D.Sc. thesis. Woods Hole Oceanogr. Inst./ Mass. Inst. Technol. Joint Program. 347 p.
- Ruderich, R. and H.H Fernholz. 1986. An experimental investigation of a turbulent shear flow with separation, reverse flow, and reattachment. J. Fluid Mech., 163: 283-322.
- Schlichting, H. 1979. Boundary-layer theory, 7th ed. McGraw-Hill, New York.
- Siegel, S. 1956. Nonparametric statistics for the behavioral sciences. McGraw-Hill, New York.

## DOCUMENT LIBRARY

March 11, 1991

### *Distribution List for Technical Report Exchange*

Attn: Stella Sanchez-Wade  
Documents Section  
Scripps Institution of Oceanography  
Library, Mail Code C-075C  
La Jolla, CA 92093

Hancock Library of Biology &  
Oceanography  
Alan Hancock Laboratory  
University of Southern California  
University Park  
Los Angeles, CA 90089-0371

Gifts & Exchanges  
Library  
Bedford Institute of Oceanography  
P.O. Box 1006  
Dartmouth, NS, B2Y 4A2, CANADA

Office of the International  
Ice Patrol  
c/o Coast Guard R & D Center  
Avery Point  
Groton, CT 06340

NOAA/EDIS Miami Library Center  
4301 Rickenbacker Causeway  
Miami, FL 33149

Library  
Skidaway Institute of Oceanography  
P.O. Box 13687  
Savannah, GA 31416

Institute of Geophysics  
University of Hawaii  
Library Room 252  
2525 Correa Road  
Honolulu, HI 96822

Marine Resources Information Center  
Building E38-320  
MIT  
Cambridge, MA 02139

Library  
Lamont-Doherty Geological  
Observatory  
Columbia University  
Palisades, NY 10964

Library  
Serials Department  
Oregon State University  
Corvallis, OR 97331

Pell Marine Science Library  
University of Rhode Island  
Narragansett Bay Campus  
Narragansett, RI 02882

Working Collection  
Texas A&M University  
Dept. of Oceanography  
College Station, TX 77843

Library  
Virginia Institute of Marine Science  
Gloucester Point, VA 23062

Fisheries-Oceanography Library  
151 Oceanography Teaching Bldg.  
University of Washington  
Seattle, WA 98195

Library  
R.S.M.A.S.  
University of Miami  
4600 Rickenbacker Causeway  
Miami, FL 33149

Maury Oceanographic Library  
Naval Oceanographic Office  
Stennis Space Center  
NSTL, MS 39522-5001

Marine Sciences Collection  
Mayaguez Campus Library  
University of Puerto Rico  
Mayaguez, Puerto Rico 00708

Library  
Institute of Oceanographic Sciences  
Deacon Laboratory  
Wormley, Godalming  
Surrey GU8 5UB  
UNITED KINGDOM

The Librarian  
CSIRO Marine Laboratories  
G.P.O. Box 1538  
Hobart, Tasmania  
AUSTRALIA 7001

Library  
Proudman Oceanographic Laboratory  
Bidston Observatory  
Birkenhead  
Merseyside L43 7 RA  
UNITED KINGDOM

<b>REPORT DOCUMENTATION PAGE</b>	<b>1. REPORT NO.</b> WHOI-92-26	<b>2.</b>	<b>3. Recipient's Accession No.</b>
<b>4. Title and Subtitle</b> Particle Contact on Flat Plates in Flow: A Model for Initial Larval Contact			<b>5. Report Date</b> June 1992
<b>7. Author(s)</b> Elizabeth D. Garland and Lauren S. Mullineaux			<b>6.</b>
<b>8. Performing Organization Name and Address</b>  The Woods Hole Oceanographic Institution Woods Hole, Massachusetts 02543			<b>8. Performing Organization Rept. No.</b> WHOI 92-26
<b>12. Sponsoring Organization Name and Address</b>  Office of Naval Research			<b>10. Project/Task/Work Unit No.</b>
			<b>11. Contract(C) or Grant(G) No.</b> (C) N00014-89-J-1112 (G) N00014-89-J-1431
<b>15. Supplementary Notes</b>  This report should be cited as: Woods Hole Oceanog. Inst. Tech. Rept., WHOI-92-26.			<b>13. Type of Report &amp; Period Covered</b>  Technical Report
			<b>14.</b>
<b>16. Abstract (Limit: 200 words)</b>  Patterns and rates of particle contact onto flat plates in steady unidirectional flows were investigated in a laboratory flume. Plates with three leading edge configurations (faired, bluff and split) were used to generate boundary-layer flows that differed in downstream patterns of plate-ward advection, turbulence and shear stress. Particle contact onto the leading edges of all plates was consistently low in 2,5, and 10 cm s <sup>-1</sup> along-stream flow speeds. Contact was enhanced under separation eddies that formed over bluff and split plates, but was reduced at reattachment points. High contact rates appeared to correspond to a combination of local plate-ward advection, a thick boundary layer, and reduced shear stress.  Surprisingly, particle contact rates in the "non-varying" flow region further downstream on the plates varied only slightly between plate types and between flow speeds. Contact rates did, however, vary strongly with particle abundance in the flume. These results were used to develop a predictive model of passive larval contact rate onto settlement plates in known larval concentrations and free-stream flows. The contact model, when combined with larval behavioral observations, provides the basis for a more objective, quantitative method of interpreting larval settlement plates.			
<b>17. Document Analysis a. Descriptors</b>  1. boundary-layer-flow 2. larval settlement 3. particle contact  b. Identifiers/Open-Ended Terms     c. COSATI Field/Group			
<b>18. Availability Statement</b>  Approved for publication; distribution unlimited.		<b>19. Security Class (This Report)</b> UNCLASSIFIED	<b>21. No. of Pages</b> 31
		<b>20. Security Class (This Page)</b>	<b>22. Price</b>